Inorg. Chem. **2006**, *45*, 10642–10650

Incorporation, Oxidation and Pyrolysis of Ferrocene into Porous Silica Glass: a Route to Different Silica/Carbon and Silica/Iron Oxide Nanocomposites

Mariane C. Schnitzler,[†] Antônio S. Mangrich,[†] Waldemar A. A. Macedo,[‡] José D. Ardisson,[‡] and Aldo J. G. Zarbin*,[†]

Departamento de Química, Universidade Federal do Paraná, CP 19081, CEP 81531-990, Curitiba, PR, Brazil, and Laboratório de Física Aplicada, Centro de Desenvolvimento da Tecnologia Nuclear, CEP 31270-901, Belo Horizonte, MG, Brazil

Received July 15, 2006

This work reports the incorporation of ferrocene into a porous silica glass under ambient temperature and atmosphere. After or during the ferrocene incorporation, the spontaneous formation of ferricinium ions was observed by electron paramagnetic resonance (EPR), UV–visible, X-ray absorption near-edge structure (XANES), and ^{57}Fe Mössbauer measurements. It was shown that the oxidation of ferrocene molecules to ferricinium ions was promoted by air and that the Si–O$^-$ groups on the surface of the pores act as counteranions. Pyrolysis of the porous glass/ferricinium material under argon atmosphere and variable temperature yields different glass/carbon nanocomposites, which were subsequently treated with an HF solution in order to remove the glassy fraction. The resulting insoluble carbon materials were characterized by transmission electron microscopy (TEM), Raman, and EPR spectroscopy and consisted of amorphous carbon when the pyrolysis was carried out at 900 or 1000 °C and of a mixture of carbon nanotubes and carbonaceous materials at a pyrolysis temperature of 1100 °C. When the pyrolysis was conducted under air, the incorporated ferricinium forms α-Fe_2O_3, and the resulting material is a transparent and highly homogeneous glass/iron oxide nanocomposite.

Introduction

The immobilization of ferrocene [iron bis(cyclopentadienyl)] into several inorganic matrices, such as zeolites, layered and porous materials, and oxide surfaces, among others, has been motivated by the potential application of these materials in fields such as catalysis, sensors, optical devices, etc.[1−14] It is well-known that loading ferrocene and other organometallic compounds into inorganic layered or porous matrices leads to materials in which the chemical and physical properties of both the matrix and the organometallic guest are often modified. These novel phenomena related to molecules confined in limited spaces can be attributed to possible chemical reactions enabled by the interactions between the guest molecules and the pore/layer wall, and/or to the anisotropic physical properties caused by the geometric

* To whom correspondence should be addressed. E-mail: aldo@quimica.ufpr.br. Tel: +55-41-33613176. Fax: +55-41-33613186.
† Universidade Federal do Paraná.
‡ Centro de Desenvolvimento da Tecnologia Nuclear.

(1) Lund, A.; Nicholson, D. G.; Lamble, G.; Beagley, B. *J. Mater. Chem.* **1994**, *4*, 1723−1730.
(2) Wong, S.-T.; Lee, J.-F.; Cheng, S.; Mou, C.-Y. *Appl. Catal. A* **2000**, *198*, 115−126.
(3) Ozin, G. A.; Godber, J. *J. Phys. Chem.* **1989**, *93*, 878−893.
(4) Mohanambe, L.; Vasudevan, S. *Inorg. Chem.* **2005**, *44*, 2128−2130.
(5) Morlat-Thérias, S.; Mousty, C.; Palvadeau, P.; Molinié, P.; Léone, P.; Rouxel, J.; Taviot-Ghého, C.; Ennaqui, A.; Roy, A.; Besse, J. P. *J. Solid State Chem.* **1999**, *144*, 143−151.
(6) Kemner, E.; Overweg, A. R.; van Eijick, L.; Fitch, A. N.; Suard, E.; de Schepper, I. M.; Kearley, G. J. *J. Chem. Phys.* **2002**, *116*, 10838−10845.
(7) Li, L.; Shi, J.-l.; Yan, J.-n.; Zhao, X.-g.; Chen, H.-g. *Appl. Catal. A: Gen.* **2004**, *263*, 213−217.
(8) Kukulka-Walkiewicz, J.; Opallo, M. *Solid State Ionics* **2003**, *157*, 263−267.
(9) Pandey, P. C.; Upadhyay, S.; Shukla, N. K.; Sharma, S. *Biosens. Bioelectron.* **2003**, *18*, 1257−1268.
(10) Opallo, M.; Kukulka-Walkiewicz, J. *Electrochim. Acta* **2001**, *46*, 4235−4242.
(11) Kaiser, C. T.; Gubbens, P. C. M.; Kemner, E.; Overweg, A. R.; Jayasooriya, U. A.; Cottrel, S. P. *Chem. Phys. Lett.* **2003**, *381*, 292−297.
(12) Zhang, F.-F.; ean, Q.; Wang, X.-L.; Sun, Z.-D.; Zhu, Z.-Q.; Xian, Y.-Z.; Jin, L.-T.; Yamamoto, K. *J. Electroanal. Chem.* **2004**, *571*, 133−138.
(13) Toda, Y.; Ishimaru, S.; Ikeda, R.; Mitani, T.; Kitao, S.; Seto, M. *J. Phys. Chem. Solids* **2004**, *65*, 471−473.
(14) Dutta, P. K.; Thomson, M. A. *Chem. Phys. Lett.* **1986**, *131*, 435−437.

10.1021/ic061312r CCC: $33.50
Published on Web 11/24/2006

constraints imposed on the guest molecular arrangements.[13] For these reasons, an understanding of the kind of host−guest interactions and the spatial orientation of the guest molecules in the voids of the host matrix are important factors that have gained considerable attention, motivated by possible applications of these systems.[3]

The utilization of porous glasses as inorganic matrices for the incorporation of organometallic compounds has been reported by numerous groups, with the purpose of obtaining new catalysts and materials for use in optical devices.[15−23] For example, different porphyrines and similar molecules have been incorporated into porous glasses, yielding heterogeneous catalysts with better performances than what is observed for the homogeneous catalysis using the neat porphyrines.[17,18] Photo- and thermosensitive organometallic compounds such as $[Fe(CO)_5]$, $[(CH_3)_3SnI]$, $[M(CO)_6]$ (M = Cr, Mo, W), $[Co_2(CO)_8]$, $[M_2(CO)_{10}]$, and $[M_3(CO)_{12}]$, among others, were impregnated and thermal- or photodegraded, in attempts at obtaining new vitreous materials that present significant refraction index variations.[16,19−23] In all these examples, an understanding of the interactions between the guest organometallic molecules and the pore walls of the glassy hosts was pivotal in explaining the observed properties of the final materials.

Porous glasses containing pores of nanometric size have also been used as host matrices for the in situ formation of nanoentities (nanoparticles, nanowires, nanoclusters, etc.) of several materials, like metals, semiconductors, oxides, and polymers.[16,24−31] In these cases, pore sizes limit particle growth. The use of a host matrix to obtain these nanoentities offers the possibility of forming new nanocomposite materials, with properties that differ from those of their individual components.[16,24−31]

One of the most commonly used glasses for these applications is the so-called porous Vycor glass, PVG (Corning 7930). This transparent porous material is obtained by acid leaching of a phase-separated alkaline borosilicate glass. The soluble borate phase is dissolved, leaving an open porous structure of essentially pure silica with interconnecting pores with a size distribution between 20 and 200 Å and a pore volume of nearly 28%.[32,33] The pore surface contains slightly acidic silanol groups. The structure of this porous glass can be consolidated upon heating to 1200 °C, at which temperature the pores collapse to form a dense, high-silica-content glass.[32,33]

In recent years, we have become interested in the synthesis, characterization, study of properties, and applications of a great number of novel porous silica glass-based nanocomposites containing different nanomaterials inside the glass pores, such as the conducting polymers polypyrole and polyaniline,[28,29] organometallic compounds,[16−18] oxides,[16,30] insulating polymers,[31] carbon,[31] and semiochemicals,[34] among others. In this paper we report the incorporation and pyrolysis of ferrocene into PVG pores. Our motivation was based on the fact that pyrolysis of ferrocene in argon atmosphere yields a very large amount of carbon nanotubes (CNT).[35−37] We reported very recently a route to iron- and iron oxide-filled CNT using ferrocene as precursor.[38] The immobilization of ferrocene into the nanometric pores of the porous Vycor glass (PVG) was carried out aiming at the growth of CNT or different structures of carbon inside the pores of PVG after the pyrolysis step, yielding novel silica glass/carbon nanocomposites.

Experimental Section

Chemicals. Acetone (Merck), hexane (Merck), fluoric acid 48% (w/w) aqueous solution (Erfran), and hydrochloric acid (Merck) were used as received. Ferrocene (Fluka) was purified by sublimation before use. Water was distilled and Milli-Q deionized before use. The PVG plates (Corning 7930) were cut into pieces measuring $10 \times 10 \times 1$ mm and treated in order to remove impurities adsorbed on their pores. The plates were immersed in a 2 mol·L^{-1} HCl solution for 30 min, washed with deionized water, dried, immersed in acetone for 30 min, dried, left at 550 °C for 72 h, cooled to room temperature, and stored in a desiccator prior to use.

Impregnation Procedure. Impregnation of PVG with ferrocene was carried out by placing a PVG plate of known weight in 20 mL of a saturated *n*-hexane solution of ferrocene for 2 h, at room temperature. After this period, the glass plate was removed from the solution and washed several times with *n*-hexane to remove

(15) Vanderspurt, T. H.; Turkevich, J.; Che, M.; Buchler, E. *J. Catal.* **1974**, *32*, 127−136.
(16) Zarbin, A. J. G.; Vargas, M. D.; Alves, O. L. *J. Mater. Chem.* **1999**, *9*, 519−524.
(17) Caiut, J. M. A.; Nakagaki, S.; Friedermann, G. R.; Drechsel, S. M.; Zarbin, A. J. G. *J. Mol. Catal. A: Chem.* **2004**, *222*, 213−222.
(18) Nakagaki, S.; Ramos, A. R.; Benedito, F. L.; Peralta-Zamora, P. G.; Zarbin, A. J. G. *J. Catal. A: Chem.* **2002**, *185*, 203−210.
(19) Sunil, D.; Sokolov, J.; Rafailovich, M. H.; Duan, X.; Gafney, H. D. *Inorg. Chem.* **1993**, *32*, 4489−4490.
(20) Gafney, H. D.; Xu, S. P. *Inorg. Chim. Acta* **1995**, *240*, 645−651.
(21) Simon, R. C.; Gafney, H. D.; Morse, D. L. *Inorg. Chem.* **1985**, *24*, 2565−2570.
(22) Borrelli, N. F.; Morse, D. L. *Appl. Phys. Lett.* **1983**, *43*, 992−993.
(23) Sunil, D.; Sokolov, J.; Rafailovich, M. H.; Kotyuzhanskii, B.; Gafney, H. D.; Wilkens, B. J.; Harson, A. L. *J. Appl. Phys.* **1993**, *74*, 3768−3777.
(24) Moreno, E. M.; Zayat, M.; Morales, M. P.; Serna, C. J.; Roig, A.; Levy, D. *Langmuir* **2002**, *18*, 4972−4978.
(25) Amekura, H.; Umeda, N.; Takeda, Y.; Lu, J.; Kishimoto, N. *Appl. Phys. Lett.* **2004**, *85*, 1015−1017.
(26) Zayat, M.; del Monte, F.; Morales, M. P.; Rosa, G.; Guerrero, H.; Serna, C. J.; Levy, D. *Adv. Mater.* **2003**, *15*, 1809−1812.
(27) Caizer, C.; Savii, C.; Popovici, M. *Mater. Sci. Eng. B* **2003**, *97*, 129−134.
(28) Maia, D. J.; Zarbin, A. J. G.; De-Paoli, M. A.; Alves, O. L. *Adv. Mater.* **1995**, *7*, 792−794.
(29) Zarbin, A. J. G.; De-Paoli, M. A.; Alves, O. L. *Synth. Met.* **1999**, *99*, 227−235.
(30) Menezes, W. G.; Camargo, P. H. C.; Oliveira, M. M.; Evans, D. J.; Soares, J. F.; Zarbin, A. J. G. *J. Colloid Interface Sci.* **2006**, *299*, 291−296.
(31) Zarbin, A. J. G.; Bertholdo, R.; Oliveira, M. A. F. C. *Carbon* **2002**, *40*, 2413−2422.
(32) Levitz, P.; Ehret, G.; Sinha, S. K.; Drake, J. M. *J. Chem. Phys.* **1991**, *95*, 6151−6161.
(33) Gafney, H. D. *Coord. Chem. Rev.* **1990**, *104*, 113−141.
(34) Zarbin, A. J. G.; Zarbin, P. H. G.; Tiboni, A. Brazilian Patent PI0306234-1, 2003.
(35) Sen, R.; Govindaraj, A.; Rao, C. N. R. *Chem. Phys. Lett.* **1997**, *267*, 276−280.
(36) Bai, S.; Li, F.; Yang, Q. Y.; Bai, J. *Chem. Phys. Lett.* **2003**, *376*, 83−89.
(37) Elias, A. L.; Rodríguez-Manzo, J. A.; McCartney, M. R.; Golberg, D.; Zamudio, A.; Baltazar, S. E.; López-Urías, F.; Muñoz-Sandoval, E.; Gu, L.; Tang, C. C.; Smith, D. J.; Bando, Y.; Terrones, H.; Terrones, M. *Nano Lett.* **2005**, *5*, 467−472.
(38) Schnitzler, M. C.; Oliveira, M. M.; Ugarte, D.; Zarbin, A. J. G. *Chem. Phys. Lett.* **2003**, *381*, 541−548.

any ferrocene absorbed on the external surface of the glass plate. The solvent incorporated during the impregnation process was removed under vacuum ($P < 10^{-3}$ Torr). During the incorporation, the transparent and colorless PVG plate gradually acquires the yellow color of the ferrocene solution, and after approximately 30 min the color gradually changes to green, staying dark green at the end of the process.

A similar incorporation procedure was done under argon atmosphere, by standard Schlenk techniques. In this procedure, the same volume of ferrocene solution exactly as described before was prepared under argon and added to a PVG plate that was pretreated under vacuum for 6 h and kept under argon. The PVG plate was maintained in the ferrocene solution for 2 h. As observed during the impregnation procedure carried out in air, the PVG plate becomes yellow after few minutes, but in contrast, it maintained this color until the end of the process. When the process was finished, the plate was removed from solution, washed several times with hexane (under Ar atmosphere), and dried under vacuum for 2 h. All samples obtained through the incorporation of ferrocene into PVG will be generically referred to here as PVG/Fc-atmosphere-time. For example, the sample PVG/Fc-air-2 h corresponds to the sample obtained under air and with the PVG plate immersed for 2 h in the ferrocene solution. Three samples will be more deeply discussed in this work: PVG/Fc-air-2 h (dark green); PVG/Fc-air-20 min (yellow), and PVG/Fc-Ar-2 h (yellow).

Ferricinium ion containing nitrate as counteranion was prepared by dissolving 0.1 g of ferrocene in 10 mL of a 5 mol·L^{-1} HNO_3 aqueous solution. The green solution obtained was maintained under stirring for 1 h and subsequently treated under vacuum until the solvent was completely removed. The incorporation of ferricinium ions into PVG was done by adding a PVG plate to the ferricinium aqueous solution for 2 h (in air), followed by washing several times with water and drying under vacuum for 4 h. The PVG plates were green after this step and will be referred here as PVG/Fc^+.

Pyrolysis. In order to perform pyrolysis of the impregnated samples (PVG/Fc-air-2 h and PVG/Fc-Ar-2 h), a quartz tube (36 mm diameter and 750 mm length) was placed in a tubular furnace and argon (99.8% purity) was passed through the tube. The impregnated PVG plates were placed inside the quartz tube in the central region of the furnace. The flow rate of the argon was controlled at 260 mL·min^{-1}. The system was maintained at room temperature and under the argon flow for 10 min, and subsequently the temperature was raised to the target value at a heating rate of 5 °C·min^{-1}. The system was kept at the final temperature (900, 1000, or 1100 °C) for 3 h, and subsequently turned off and cooled to room temperature at an approximate rate of 25 °C·min^{-1}. The samples were removed and stored in a desiccator. The samples obtained through pyrolysis of sample PVG/Fc-air-2 h at 900, 1000, and 1100 °C will be refereed here as PVG/C-900, PVG/C-1000, and PVG/C-1100, respectively.

The heat treatment of the PVG/Fc-air-2 h sample in air was done by exactly the same procedure, but with an air flow of 260 mL−min^{-1}. The resulting sample will be referred as PVG/oxide.

The materials resulting from pyrolysis in argon atmosphere (samples PVG/C-900, PVG/C-1000, and PVG/C-1100) were stirred in a 48 wt % aqueous HF solution for 2 days (***Caution:*** *HF is very dangerous and all manipulation should be done while wearing gloves and under a fume hood*). The resulting insoluble materials were retrieved by centrifugation and washed exhaustively with deionized water. The material resulting from the HF treatment of samples PVG/C-900, PVG/C-1000, and PVG/C-1100 will be designated as C-900, C-1000, and C-1100, respectively.

The amount of ferrocene incorporated, as well as the yield of carbon resulting from the pyrolysis step, were estimated by gravimetric measurements.

Characterization of Samples. UV−vis−NIR absorption spectra were collected directly from the glass plates in a Scinco S-1150 spectrophotometer, using air as reference, in the 200−900 nm range.

Raman spectra were measured in a Renishaw Raman image spectrophotometer, coupled to an optical microscope that focused the incident radiation in a 1 μm spot, by use of a 514 nm laser as the excitation source and 20 mW power. Spectra were obtained from 30 scans, over the 2000−200 cm^{-1} region.

EPR spectra were obtained in ground samples, at room temperature or at 77 K, in quartz tubes. A Bruker ESP 300E spectrometer was used, operating at a frequency of ∼9.5 GHz (X-band), with a 100 kHz modulation frequency, 10.145 G modulation amplitude, and 2 mW microwave power.

X-ray diffraction measurements were done in a Shimadzu XD-3A diffractometer using Cu Kα radiation, with 40 kV and 40 mA, at 0.02° scan rate (in 2θ). Powder silicon reflections were used for 2θ calibration.

The transmission Mössbauer spectra were obtained in a CMTE model MA250 spectrometer with a ^{57}Co/Rh source at room temperature. Mössbauer isomer shifts are quoted relative to α-Fe.

Transmission electron microscopy (TEM) was done in a JEOL JEM 120 KV instrument. A dispersion of the samples in acetonitrile was prepared and sonicated for 5 min. The dispersion was allowed to set for 10 min, and a drop of this dispersion was added over a standard holey copper grid covered by a thin carbon film.

The X-ray absorption spectroscopy (XAS) experiments were performed on the XAS beam line of the Laboratório Nacional de Luz Síncrotron (LNLS, Brazil). Extended X-ray absorption fine structure (EXAFS) and X-ray absorption near-edge structure (XANES) spectra were collected at the iron K-edge (7112 eV) by use of a Si (111) monochromator calibrated in the K edge of metallic iron. Solid ferrocene, metallic iron, and α-Fe_2O_3 were used as reference compounds. The experimental XANES spectra were collected with a resolution around of around 0.3 eV, background-corrected by use of a Victoreen fit, and normalized with the program WINXAS. The EXAFS spectra were analyzed and fitted by use of the WINXAS code.

The sequence of impregnation, pyrolysis, HF treatment of the samples, and the main experimental evidence obtained from this work is represented in Figure 1. The details of each step will be presented in the text.

Results and Discussion

Incorporation of Ferrocene into Porous Silica Glass. When the porous glass plate is introduced into ferrocene solution, diffusion of the ferrocene to the interior of the glass pores occurs through a capillarity process, as reported previously for the incorporation of different neutral molecules in PVG.[39,40] The adsorbed material on the external surface of the glass plate was removed through several washing steps, and the co-impregnated solvent was eliminated trough the treatment of the material under low pressure. The amount of ferrocene impregnated into a PVG plate can be varied controlling the concentration of the ferrocene solution, the temperature at which the impregnation is carried out, and the time for which the PVG plate is maintained immersed

(39) Straley, C.; Matteson, A.; Feng, S.; Schwartz, L. M.; Kenyon, W. E.; Banavar, J. R. *Appl. Phys. Lett.* **1987**, *51*, 1146−1148.
(40) Okubo, T.; Inoue, H. *J. Chem. Eng. Jpn.* **1987**, *20*, 590−597.

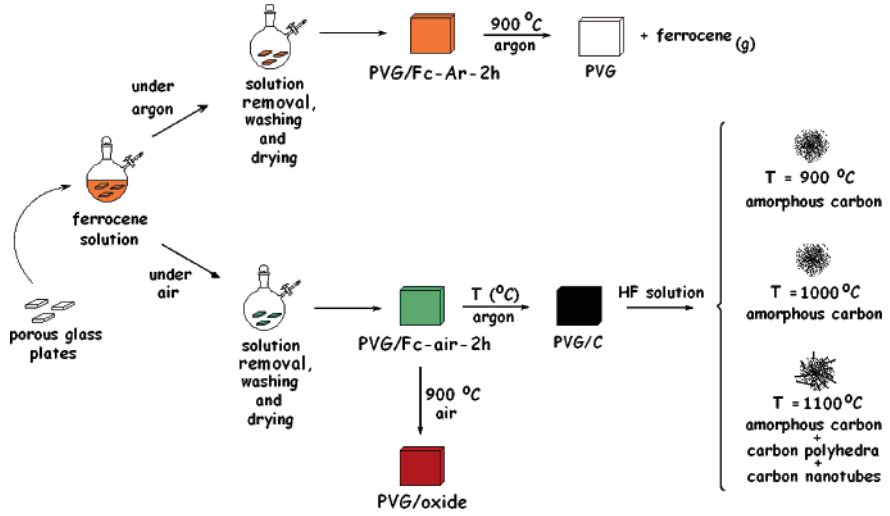

Figure 1. Schematic summary of the routes to different silica/carbon and silica/iron oxide nanocomposite materials described in this work, based on the impregnation and pyrolysis of ferrocene into porous glasses. For details, see text.

on the ferrocene solution. In the conditions used to prepare the sample PVG/Fc-air-2 h, the amount of impregnated ferrocene was approximately 1.8×10^{-3} g of ferrocene/g of PVG (9.63×10^{-6} mol of ferrocene/g of PVG). This amount increased to 6.05×10^{-2} g of ferrocene/g of PVG (3.24×10^{-4} mol of ferrocene/g of PVG) when the impregnation process was conducted for 72 h at room temperature.

As described in the Experimental Section, during the incorporation of ferrocene carried out in air, the PVG plate becomes green after 30 min. This effect occurs with no changes to the color of the ferrocene solution in which the PVG plate is dipped. The absorption spectra of the ferrocene solution are almost the same (except for a decrease in the absorbance intensity, due the reduction in the concentration of the ferrocene solution during the impregnation step) before and after the impregnation process, indicating that no ferrocene degradation occurred (as expected, because it is well-known that ferrocene, both solid or in solution, is highly stable in air).

The green color observable on the PVG/Fc-air-2 h sample is characterized by a band at 615 nm on the absorption spectrum, as can be seen in Figure 2. Figure 2a shows the UV−vis spectrum of one plate of neat PVG. As we can see, the PVG is almost transparent in the visible region. The ferrocene solution used in the impregnation process has the UV−vis spectrum shown in Figure 2b, which is characteristic of the reported spectrum for ferrocene:[41] one band at 435 nm, one band at 320 nm, and one band at 261 nm. Figure 2c shows the absorption spectrum of a PVG/Fc-air-20 min sample. Note that the green color was not formed yet in this sample, due to the reduced time in which the PVG plate was maintained dipped in the ferrocene solution. As previously reported for other PVG-incorporated organometallic compounds,[16,19] the UV−vis absorption spectra of the ferrocene in solution and inside the PVG pores (PVG/Fc-air-20 min sample) are very similar, showing that the

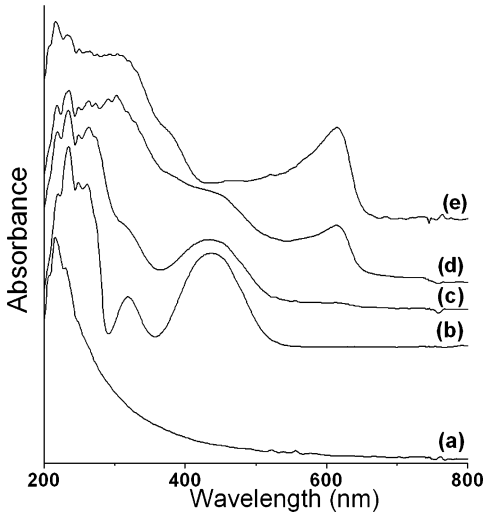

Figure 2. UV−Vis absorption spectra: (a) neat PVG; (b) hexane ferrocene solution; (c) sample PVG/Fc-air-20 min; (d) sample PVG/Fc-air-2 h; (e) sample PVG/Fc^+.

ferrocene incorporation was successfully done without distortion or destruction of the molecular structure of this compound.

The spectrum of the PVG/Fc-air-2 h (therefore the green PVG/Fc) is presented in Figure 2d. The remarkable band at 615 nm observable in this spectrum is characteristic of the ferricinium cation $[Fe(C_5H_5)_2]^+$, obtained from the oxidation of the ferrocene.[41,42] The occurrence of this band could indicate that the green color of PVG/Fc-air-2 h sample is due to an oxidation of the impregnated ferrocene inside the PVG pores. In order to verify this hypothesis, we prepared a ferricinium cation as described in the Experimental Section and conducted the impregnation of this cation into the PVG. The spectrum of this PVG/Fc^+ material is presented in Figure 2e, and it is very similar to the spectrum of Figure 2d. The oxidation of ferrocene inside the pores of PVG was confirmed by other characterization techniques and will be discussed later.

(41) Sohn, Y. S.; Hendrickson, D. N.; Gray, H. B. *J. Am. Chem. Soc.* **1971**, *93*, 3603−3612.

(42) Aoi, N.; Matsubayashi, G. E.; Tanaka, T. *Polyhedron* **1987**, *6*, 943−946.

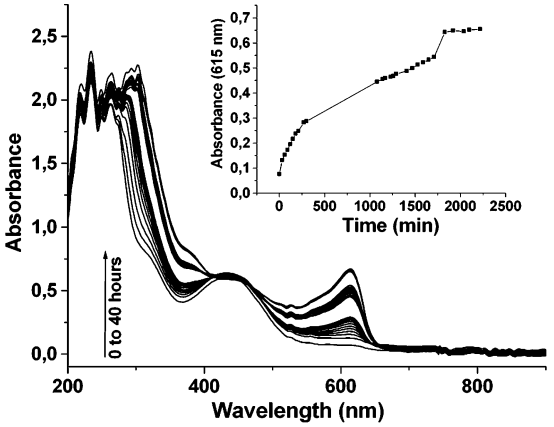

Figure 3. UV−Vis absorption spectra of a PVG/Fc-air-20 min sample kept in air. The spectra were collected directly from the sample at different time intervals (see text). (Inset) Evolution of intensity of the 615 nm band with time.

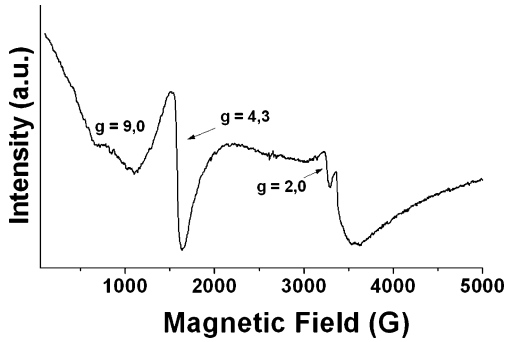

Figure 4. EPR spectrum of the PVG/Fc-air-2 h sample recorded at 77 K.

A very interesting effect observable on the PVG/Fc-air-20 min sample is that the evolution of the green color also occurs if the sample is maintained out of the ferrocene solution. This means that after performing all the procedures (incorporation, washing, and drying at low pressure) to prepare a PVG/Fc-air-20 min sample, it gradually changes its color to green. This process was followed by UV−vis spectroscopy, as shown in Figure 3. In order to collect these spectra, the PVG/Fc-air-20 min sample was placed in the sample compartment of the spectrophotometer and was not changed for 40 h. Spectra were collected at different times, as illustrated in Figure 3. Zero time was defined as the time at which the sample was positioned in the spectrophotometer and the first spectrum was collected. As we can see, the spectrum at zero time is typical of the ferrocene, with no band at 615 nm. However, as time elapsed, the band at 615 nm appeared and its intensity grew considerably (and consequently the green color). This is an important result because it shows us that the process involved in the yellow−green conversion is caused by some kind of interaction between the incorporated ferrocene and the surface of the glass pores, and is not related to the contact between the PVG and the ferrocene solution but only to the ferrocene molecules that were incorporated into PVG. This consideration also will be discussed later.

Figure 4 shows the EPR spectrum of the PVG/Fc-air-2 h sample recorded at 77 K. As expected, no EPR signals were observed in the neat ferrocene or neat PVG, as well as in the PVG/Fc-air-20 min sample (data not shown). The spectrum presented in Figure 4 shows clearly a set of typical Fe^{3+} signals at $g = 9.0$ and 4.3 (corresponding to Fe^{3+} ions in high-spin and rhombic sites) and $g = 2.0$ (due to Fe^{3+} ions in a cubic structure). These g values indicate the occurrence of Fe^{3+} in dilute domains (with no $Fe^{3+}-Fe^{3+}$ interactions) in two different chemical environments and are comparable to the reported values for ferricinium ions formed by the oxidation of ferrocene molecules adsorbed in MCM-41 framework.[13] The EPR data shown in Figure 4 confirm definitely that the ferrocene molecules are oxidized after their incorporation into PVG pores.

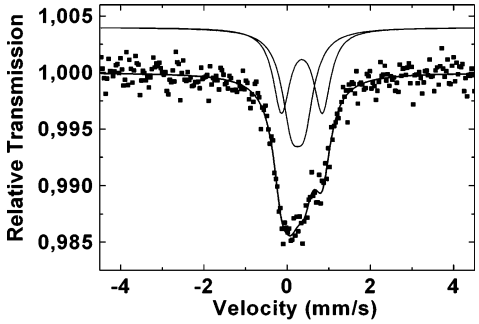

Figure 5. ^{57}Fe Mössbauer spectrum of the PVG/Fc-air-2 h sample.

^{57}Fe Mössbauer spectroscopy was employed to determine the chemical state of iron atoms in the PVG/Fc-air-2 h sample. As shown in Figure 5, the Mössbauer spectrum at room temperature is characterized by a broad asymmetric peak corresponding to Fe^{3+} ions in two nonequivalent sites. Our Mössbauer results indicate clearly that the iron atoms are completely oxidized to ferricinium ions. The presence of ferrocene (typically a doublet with isomer shift ~0.40 mm·s^{-1} and quadrupole splitting ~2.40 mm·s^{-1}, corresponding to resonance lines around 1.6 and −0.8 mm·s^{-1})[43,44] is ruled out.

Figure 6 shows the pre-edge region of the XANES spectrum of a PVG/Fc-air-2 h sample (Figure 6b), collected at iron K-edge. The XANES spectra of ferrocene (Figure 6a), α-Fe_2O_3 (Figure 6c), and metallic iron (Figure 6d), used as standards, are also shown. As we can see, there are no strong differences between the ferrocene and PVG/Fc-air-2 h spectra. All the peaks labeled A, B, C, and D are characteristic of the ferrocene.[45] Pre-edge peak A corresponds to a forbidden Fe 1s → 3d transition.[46] The position of this pre-edge peak is sensitive to the iron valence.[46] The energy of this peak for the PVG/Fc-air-2 h sample (Figure 6b) is the same as for the α-Fe_2O_3 standard sample (Figure 6c) and is shifted 2 eV to higher energy when compared with the spectrum of pure ferrocene (Figure 6a), indicating the increase of the formal oxidation state of the iron in the PVG/Fc-air-2 h sample. Again, these results are compatible with

(43) Schwerdtfeger, P.; Söhnel, T.; Pernpointner, M.; Laerdahl, J. K.; Wagner, F. F. *J. Chem. Phys.* **2001**, *115*, 5913−5924.
(44) Wertheim, G. K.; Herber, R. H. *J. Chem. Phys.* **1963**, *38*, 2106−2111.
(45) Ruiz-Lopez, M. F.; Loos, M.; Goulon, J.; Benfatto, M.; Natoli, C. R. *Chem. Phys.* **1988**, *121*, 419−437.
(46) Wong, S.-T.; Lee, J.-F.; Cheng, S.; Mou, C.-Y. *Appl. Catal. A: Gen.* **2000**, *198*, 115−126.

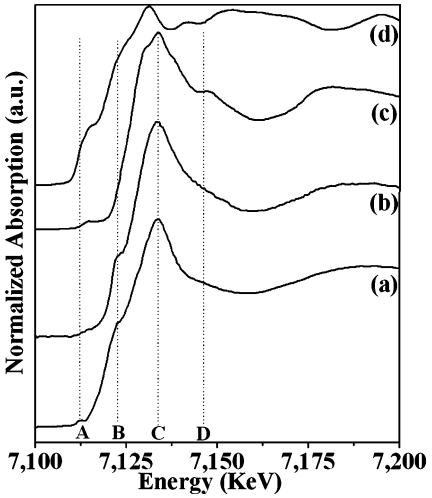

Figure 6. Iron K-edge X-ray absorption spectra: (a) neat ferrocene; (b) sample PVG/Fc-air-2 h; (c) α-Fe_2O_3; (d) iron foil.

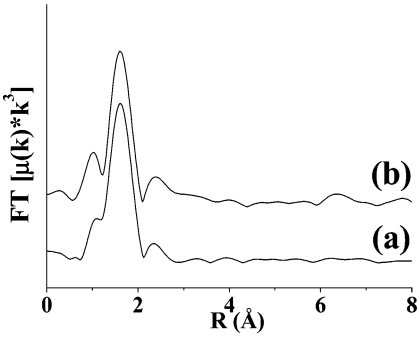

Figure 7. Normalized magnitude Fe K-edge FT-EXAFS spectra of neat ferrocene (a) and sample PVG/Fc-air-2 h (b).

the previous data and corroborate the ferricinium occurrence in the PVG/Fc-air-2 h samples.

The experimental EXAFS spectra were fitted and Fourier transformed (Figure 7). The ferrocene and PVG/Fc-air-2 h curves are very similar. Only one prominent peak is found in the Fourier transformed curves for theses samples, attributed to Fe−C scattering path. The best-fit EXAFS data of the PVG/Fc-air-2 h sample are the following: iron coordination number $N = 10.78$, Fe−C intramolecular bond length $R = 2.045$ Å, and Debye−Waller factor $\sigma^2 = 1.5 \times 10^{-4}$ Å.[2] The coordination number of the iron and the Fe−C intramolecular bond length in the PVG/Fc-air-2 h are a little bit different from what is observed for the pure ferrocene ($N = 10$ and $R = 2.047$ Å), as reported for ferricinium cation.[47]

According to the results presented until now, it is clear that after the incorporation process, the ferrocene was oxidized to ferricinium inside the PVG pores. However, we did not discuss yet who acts as oxidizing agent in this process. Based on the experimental evidence, specifically on the fact that the oxidation process occurs regardless of whether the PVG plate remains dipped in the ferrocene solution or kept in air, we supposed that the ferrocene oxidation was done by air. Although this hypothesis should looks like improbable at first (since, as we said before, ferrocene is very stable in air), it is necessary to remember that the surface of the PVG pores is formed by a high concentration of acid silanol groups, and it is known that ferrocene is oxidized by air in the presence of acids. To verify the influence of the air on the oxidation of impregnated ferrocene, we carried out an immobilization process under argon atmosphere. As we expected, the green color was not formed after 50 h of impregnation. The sample had an intensely yellow color and the UV−vis spectrum (not shown) present only the ferrocene bands, confirming that the oxygen, in the presence of the silanol groups from the PVG surface, is responsible for the ferrocene oxidation inside the PVG pores. The net oxidation reaction should be represented as follows:

$$2 \equiv Si{-}O{-}H + 2Fe(C_5H_5)_2 + \frac{1}{2}O_2 \rightarrow 2 \equiv Si{-}O^{-}Fe(C_5H_5)_2^{+} + H_2O$$

By this representation, the $Si{-}O^{-}$ remaining on the surface of the PVG pores acts as counteranion to stabilize the ferricinium cation. This fact is supported by infrared spectroscopy, in which the strong and sharp band at 3740 cm^{-1}, observable in the neat PVG spectrum and attributed to the O−H stretching from the surface silanol groups, disappears in the PVG/Fc-air-2 h spectrum, indicating that the Si−O−H bonding no longer exists after the impregnation and oxidation of ferrocene into PVG (spectra not showed).

Pyrolysis of Sample PVG/Fc. The PVG/Fc-air-2 h sample was heat-treated at different temperatures in both air and argon atmosphere. The samples obtained from the pyrolysis of the PVG/Fc-air-2 h under argon atmosphere (samples PVG/C) showed a black color typical of carbon formation. The sample PVG/Fc-Ar-2 h was also pyrolyzed. However, in contrast to results for the previously mentioned sample, the resulting material was transparent and colorless, similar to the neat PVG. This indicates that the impregnated ferrocene was sublimated during the heat treatment, as expected for "free" ferrocene. These data suggest that ferrocene interacts weakly with the surface of the PVG pores. On the other hand, when the ferrocene oxidation took place, the resulting ferricinium cations interact strongly with the surface of PVG pores (as outlined by the oxidation reaction represented before), and the heat treatment occurs with small or no losses of the impregnated compound by sublimation, resulting in a carbon structure inside the pores of PVG. Due to its high thermal stability, PVG remains stable after heat treatment at 900−1100 °C. At these temperatures, the silanol groups present on the pore walls are condensed to form water, and the pore structure remains open.[32−34] These new PVG/C nanocomposites are dark black and represent new penetrating carbon/silica hybrid materials.

The treatment of the PVG/C samples with HF solution dissolves the glassy fraction, resulting in an insoluble carbon material. By gravimetric control of the insoluble carbon resulting from the HF treatment of sample C-900, it was possible to estimate the amount of approximately 4.48×10^{-4} g of carbon/g of PVG, which represents a carbon yield

(47) Chernov, V. A.; Nikitenko, S. G.; Danilenko, A. M. *Nucl. Instrum. Methods Phys. Res. A* **1995**, *359*, 248−249.

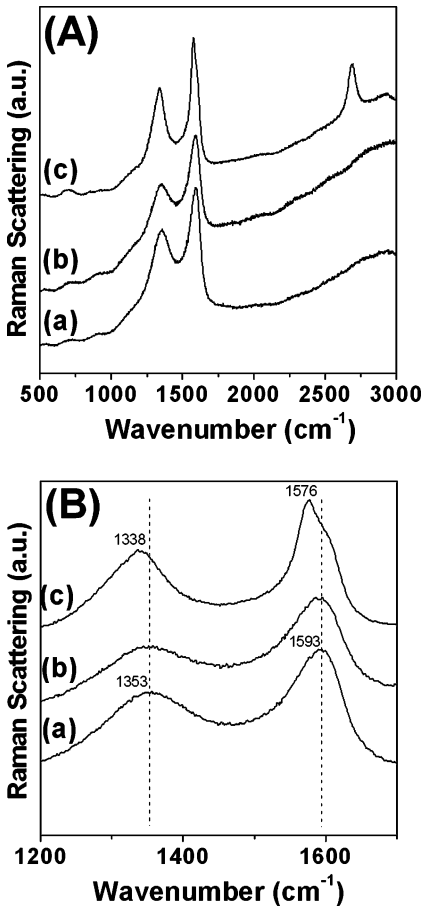

Figure 8. (A) Raman spectra of the samples: (a) C-900, (b) C-1000, and (c) C-1100. (B) Detail of the same spectra presented in panel A.

of 38.8% (considering 1.8×10^{-3} g of ferrocene previously impregnated for each gram of PVG). It is important to note that the gravimetric control of all these processes is not trivial, since a significant fraction of weight losses should be attributed to the water, resulting from the temperature-induced condensation of silanol groups present on the surface of the PVG pores. In this way, the carbon yield of this process should be higher than what was presented above. Also, the amount of carbon produced can be increased by an increase in the previous amount of ferrocene incorporated into PVG, as described before.

Figure 8 shows the Raman spectra of samples C-900, C-1000, and C-1100 (Figure 8, spectra a, b and c, respectively). Two main Raman modes are observable in all the spectra in Figure 8, at about 1590 and 1350 cm^{-1}. The band at about 1590 cm^{-1} is referred to as the G band and was attributed to the E_{2g} mode of graphite.[48] The band at about 1350 cm^{-1} is referred to as the D band and was attributed to a disordered-induced line due to small particle size effect or lattice distortion.[49] Figure 8B shows in detail the D and G bands on the Raman spectra of the samples. The D and G bands are present in various sp^2 carbon materials, and the frequency, strength, and linewidth of these bands is found to be a function of the degree of structural disorder.[50] Shifts to lower frequency, as well as a decrease in the I_D/I_G ratio, are frequently associated with an increase in the degrees of graphitization of the carbonaceous material.

The spectra of C-900 (Figure 8, spectra a) and C-1000 (Figure 8, spectra b) present only the G and D bands, at 1593 and 1353 cm^{-1}, respectively, and are typical of disordered sp^2 carbon material. No significant differences were observable in these two spectra, indicating similar disordered structures for the carbonaceous materials formed at 900 or 1000 °C. The material formed at 1100 °C, however, present different structures, as observable in the Raman spectrum of sample C-1100 present in Figure 8, spectrum c. This spectrum presents a clear shift of the G and D bands, when compared with the product formed at lower temperatures (from 1593 and 1353 to 1576 and 1338 cm^{-1}, respectively, as observed in Figure 8B). As described before, these shifts are associated with an increase in the graphitization degree of the material. This interpretation is corroborated by the appearance of a well-defined band at 2684 cm^{-1} on the spectrum of the carbonaceous material formed at 1100 °C. This second-order Raman mode is an overtone of the D band and is characteristic of well-graphitized carbon samples, such as HOPG and single- or multiwalled carbon nanotubes.[51]

Figure 9 shows the EPR spectra of the materials resulting from the PVG/Fc-air-2 h pyrolysis, before (Figure 9, panel I) and after (Figure 9, panel II) the HF treatment. The spectrum of the sample PVG/C-900 (Figure 9, panel I, spectrum a) shows the very low-intensity Fe^{3+} line at $g = 4.3$ corresponding to rhombic Fe^{3+} and a narrow radical line at $g = 1.977$, characteristic of unpaired electrons on disordered carbon structures.[52] The free radical line is over a broad Fe^{3+} line (g around 2.0) characteristic of high-spin Fe^{3+} ions in concentrated domains, showing $Fe^{3+}-Fe^{3+}$ interactions. The spectrum of the sample PVG/C-1000 (Figure 9, panel I, spectrum b) shows an increase in the intensity of the Fe^{3+} in concentrated domains ($g = 2.4$) with a broad line ($\Delta H_{pp} = 1200$ G) indicating strong $Fe^{3+}-Fe^{3+}$ interactions, besides the free radical line as described before. In sample PVG/C-1100 (Figure 9, panel I, spectrum c) the EPR spectrum presents a typical line of Fe^{3+} ions in cubic symmetry ($g = 2.036$ and ΔH_{pp} around 400 G). The carbon free radical line should be observed in the small asymmetry of this line, as indicated by an arrow in Figure 9, panel I, spectrum c. After the HF treatment, no more Fe^{3+} signal should be detectable on the spectra of the resulting material C-900 and C-1000 (Figure 9, panel II, spectra a and b, respectively), which indicates that the iron species resulting from the pyrolysis were also solubilized through the HF treatment. The resulting materials are composed only by amorphous carbon, with the typical radical signal at $g = 1.997$.

(48) Tuinstra F.; Koenig J. L. *J. Chem. Phys.* **1970**, *53*, 1126−1130.
(49) Eklund, P. C.; Holden, J. M.; Jishi, R. A. *Carbon* **1995**, *33*, 959−972.
(50) Cuesta, A.; Dhamelincourt, P.; Laureyns, J.; Martínez-Alonso, A.; Tascón, J. M. D. *J. Mater. Chem.* **1998**, *8*, 2875−2879.
(51) Sveningsson, M.; Morjan, R.-E.; Nerushev, O. A.; Bäckström, J.; Campbell, E. E. B.; Rohmund, F. *Appl. Phys. A* **2001**, *73*, 409−418.
(52) Emmerich, F. G.; Rettori, C.; Luengo, C. A. *Carbon* **1991**, *29*, 305−311.

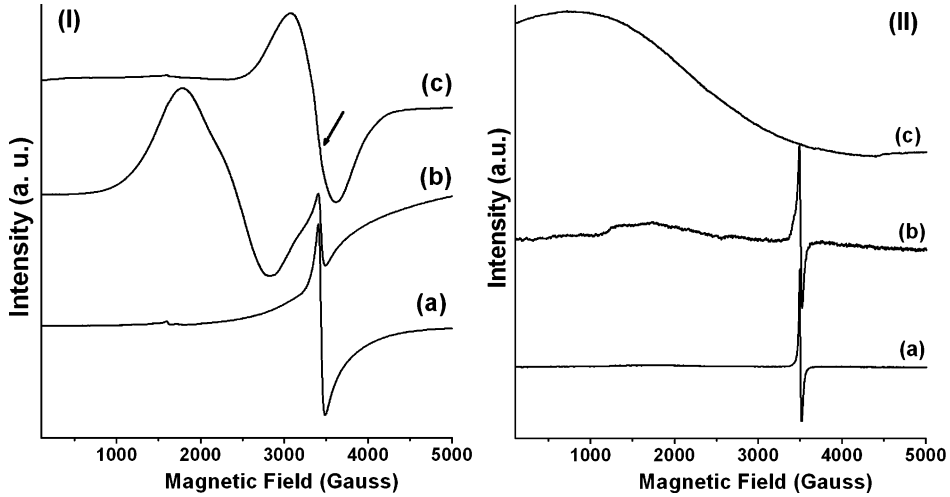

Figure 9. EPR spectra. (I) (a) PVG/C-900, (b) PVG/C-1000, and (c) PVG/C-1100. (II) (a) C-900, (b) C-1000, and (c) C-1100.

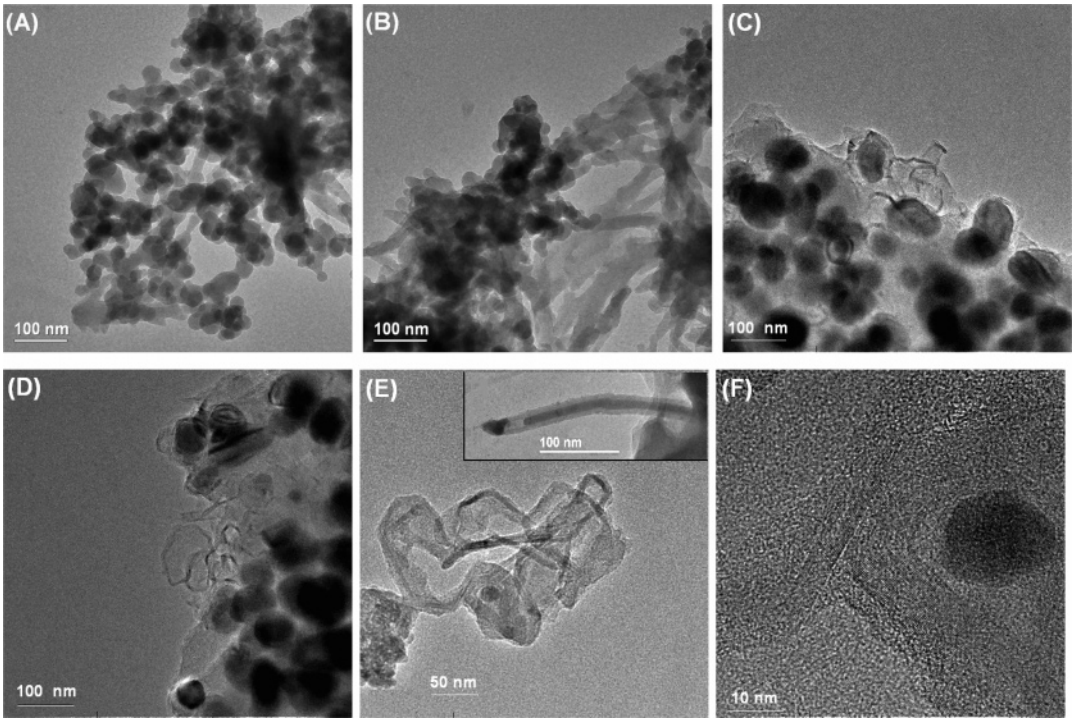

Figure 10. TEM images of the carbonaceous samples: (A, B) C-900; (C−F) C-1100.

The EPR spectrum of sample C-1100 (Figure 9, panel II, spectrum c) presents very different behavior, characterized by a strong and broad Fe^{3+} signal (ΔH_{pp} around 3000 G), which indicates strong $Fe^{3+}-Fe^{3+}$ coupling. Only this Fe^{3+} signal remained after the HF treatment, which indicates that, in contrast to the other samples, the iron species were not solubilized by the HF treatment.

The TEM images of the different carbonaceous samples are presented in Figure 10. The images corroborate the data obtained from Raman and EPR spectroscopy. As we can see, the images obtained from sample C-900 (Figure 10A,B), indicate that this sample is formed by an agglomerate of small particles of amorphous carbon. The images of sample C-1100, however, show the occurrence of short carbon nanotubes, mixed with some graphitic structures and other kind of carbonaceous material. Figure 10C,D shows dark particles embedded on a mass (probably formed by carbon) and many small carbon nanotubes. Figure 10E shows clearly the carbon nanotubes and some carbonaceous structures. The detail of Figure 10E presents one multiwalled carbon nanotube that occurs on this sample. Figure 10F present a high-resolution TEM image of a graphitic structure, in which the distance of 0.334 nm was measured between the crystal planes. It is clear in this image that the carbonaceous graphitic structure is surrounding one dark particle, related to iron species. The pictures presented in Figure 10C−10E are highly elucidative regarding the persistence of iron compounds after the HF treatment of the C-1100 sample, as observed by EPR spectroscopy. It is clear that the iron compounds are protected by the carbon structures, which obstruct the HF access.

Sample PVG/Fc-air-2 h was also heat-treated under air, aiming at ferricinium conversion to iron oxide, resulting in a glass/oxide nanoparticles composite (samples PVG/oxide).

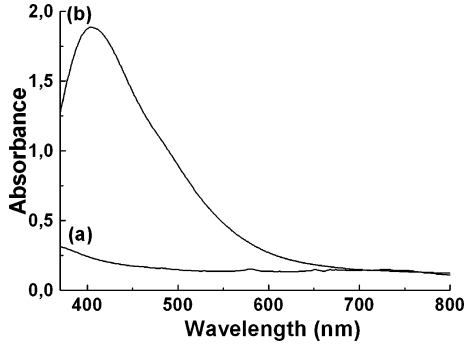

Figure 11. UV−vis absorption spectra: (a) neat PVG; (b) sample PVG/oxide.

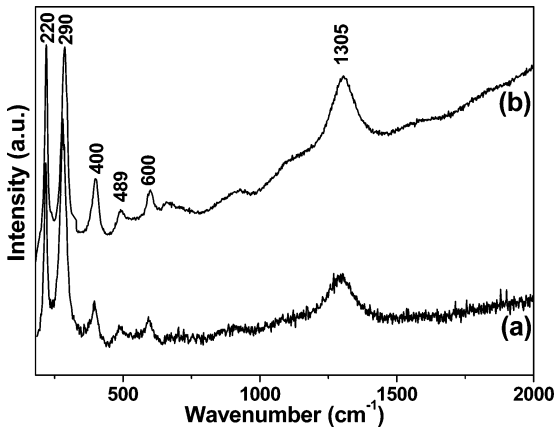

Figure 12. Raman spectra: (a) α-Fe_2O_3; (b) sample PVG/oxide.

After the heat treatment of PVG/Fc-air-2 h under air at 900 °C, the resulting product was a very homogeneous and transparent brown-red color material. The UV−vis spectra of both the neat PVG and the product of the pyrolysis of the PVG/Fc-air-2 h under air atmosphere are presented in Figure 11. The PVG/oxide spectrum presents an absorption onset at approximately 680 nm and two bands at 404 and at 470 nm (shoulder), which can be assigned to $p_\pi \rightarrow d_\pi$ ligand-to-metal charge-transfer (LMCT) transitions involving the oxide ligands and Fe^{III} centers.[53]

The impregnation and pyrolysis cycle of ferrocene inside the PVG pores can be repeated several times. It is well-known that the silanol groups on the surface of PVG pores are regenerated after the heat-treatment step, what means that it is possible to repeat the ferrocene impregnation in a sample after the pyrolysis, and repeat the pyrolysis yet again. This cycle of impregnation/pyrolysis/impregnation/pyrolysis can be performed several times, in order to increase the amount of oxide in the final material. This procedure was very important in order to characterize the iron species resulting from the heat treatment. Figure 12 shows the Raman spectrum of a sample resulting from the heat-treatment in air of a PVG/Fc-air-2 h sample (PVG/oxide, Figure 12b), in which the impregnation and pyrolysis cycle was repeated five times. All the bands presented in this spectrum were attributed to α-Fe_2O_3,[54,55] indicating that this iron oxide was formed. A spectrum of neat α-Fe_2O_3 is presented in Figure 12a for comparison. Note that the line width of the main Raman bands is larger on the PVG/oxide spectrum than on the neat oxide, probably due to the small particle size obtained inside the PVG pore structure.

Conclusion

In conclusion, this work demonstrates a very simple solid-state route to novel glass/amorphous carbon, glass/carbon nanotube, and glass/iron oxide materials, based on the incorporation and pyrolysis of ferrocene into porous glass. The oxidation of the impregnated ferrocene to ferricinium cation was considered essential to the formation of the nanocomposites, due to the strong interaction between the ferricinium and the surface of the PVG pores that retains the impregnated compound under high temperatures. A summary of the different routes to nanocomposite materials produced in this work is presented in Figure 1.

It is important to note that several attempts have been made to synthesize novel silica/carbon and silica/iron oxide nanocomposites. The routes described here are very simple and versatile, do not require a complex experimental apparatus, and probably can be extended to other metallocene compounds. Efforts to examine this possibility are in progress in our research group.

Acknowledgment. We thank CNPq, CT-ENERG/CNPq, CAPES, TWAS, Rede Nacional de Nanotubos de Carbono (MCT) and LNLS−National Synchrotron Light Laboratory, Brazil (Project XAS 1030) for financial support and Centro de Microscopia Eletrônica-UFPR, Laboratório de Microscopia Eletrônica-LNLS, and Dra. Marcela Mohallem Oliveira for the TEM images. M.C.S. thanks CAPES for the fellowship.

Supporting Information Available: Thermogravimetric data for the neat PVG and sample PVG/Fc-air-2 h. This material is available free of charge via the Internet at http://pubs.acs.org.

IC061312R

(53) Kumar, M. S.; Schwidder, M.; Grünert, W.; Brückner, A. *J. Catal.* **2004**, *227*, 384−397.

(54) Pérez-Robles, F.; García-Rodriguez, F. J.; Jiménez-Sandoval, S.; Gonzáliez-Hernández, J. *J. Raman Spectrosc.* **1999**, *30*, 1099−1104.

(55) Oh, S. J.; Cook, D. C.; Townsend, H. E. *Hyperfine Interact.* **1998**, *112*, 59−65.